

A case study of the use of large-diameter high-density polyethylene geopipes

Y. Sumiyama
High Stiffness Polyethylen Pipes Association

K. Tasiro
DaiNippon Plastics Co. Ltd.

Keywords: drainage, high-density polyethlen geopipes, high embankment, large-diameter geopipes

ABSTRACT: Presented in this paper is a case study in Kumamoto Prefecture, Kyushu, Japan, in which a large diameter (about 2 m) high-density polypropylene geopipe for drainage of stormwater from the upstream was installed across a high road embankment with a maximum depth of the backfill equal to 32 m. Due to high earth pressure that would be activated on the pipes, electric-resistance strain gauges were attached to the pipes and deflection gauges were installed in the pipes to monitor the stresses and deflections of the pipes and a number of earth pressure cells were arranged in the backfill adjacent to the piles to monitor the pressure acting on the pipes for a period from February 18, 2002 to March 19, 2003.

1 INTRODUCTION

Drainage pipes buried in the ground are often exposed to deteriorating effects of various kinds of chemicals, organic substances, abrasive sedimentary materials (mud, silt, sand and other clastic substances), hydrogen sulfide and other corrosive gases into which organic substances are biodegraded. For this reason, conventional casting pipes could be susceptible to corrosion. On the other hand, as conventional reinforced concrete pipes are heavy, each unit is made short for the convenience of transportation and handling, which increases the number of joints per stretch. This results in a significant low installation efficiency, while these joints are usually susceptible to water leakage from and into the inside of the pipes and intrusion of rhizomes.

In view of several inherent problems of the conventional type pipes as described above, high pressure-resistant drain geopipes produced by a so-called spiral winding forming process based on a unique hollow rib design were developed. These geopipes are made of high-density polyethylene, which has high chemical resistance, high wear resistance, high water tightness and lightweightness and high workability. Due to these features of the production process and the raw material, the polyethylene geopipes are characterized by a high-pressure resistance, a high rigidity and a light weightness, which results in a minimized number of joints per stretch and therefore highly efficient transportation and on-site handling. The polyethylene geopipes have

been internationally recognized, and they have been standardized in DIN 19961-1989 (Germany) and ASTM F894-1992 (U.S.A.) and enrolled in the Japanese Industrial Standards as JIS K 6780 (Pressure-Resistant Ribbed Polyethylene Pipes) in 1996.

The following two types (see Fig. 1) are available in the market:

- (1) Type R (nominal size: 300–3,000 mm in diameter), externally laced with circular or rectangular ribs wrapping-around a pipe.
- (2) Type F (nominal sizes: 200–2,000 in diameter) having smooth internal and external wall surfaces and a hollow shell.

The respective type is available in the form of straight tubes, bends, branches, stubs, and manhole joints in four different strength grades.

Pipe rigidity (kN/m ²)	30	60	90	120
Type	R R30 F F30	R60 F60	R90 F90	R120 F120
Nominal diameter (mm)	300~3000	300~2000	300~2000	200~1000

2 CASE HISTORY

2.1 Site conditions

Since the 1995 Great Kobe Earthquake (Hyogo-ken Nambu Earthquake), an efficient reduction of the

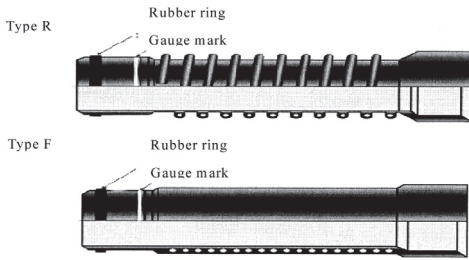


Figure 1. Two basic types of polyethylene geopipes.

damage to civil engineering infrastructures has been one of the major technical concerns. For road embankments to have a sufficiently high seismic stability, it is crucial to keep the pore water pressure

in the backfill as low as possible by effective drainage from the adjacent areas and the inside of the backfill. Presented herein is a case study in Kumamoto Prefecture, Kyushu, Japan, in which a large diameter (about 2 m) high-density polypropylene geopipe for drainage of stormwater from the upstream was installed across a high road embankment with a maximum depth of the backfill equal to 32 m.

Figure 2 shows the installation of a geopipe in the project. Figure 3 shows the specifications of the geopipe used in this project. The geopipe was placed in an excavated ditch, as shown in Fig. 4a, at the bottom of the road embankment.

A compaction test of the backfill soil was performed in the laboratory. The soil conditioner was added at a rate of 65 kg/m³ as determined by the indoor unconfined compression test.

Table 2. Specifications of the geopipe used in the project (all the unit: mm).

Nominal size	Internal diameter	Effective length	Male end				Female end				Reference value			
			External diameter		Length		Inside diameter		Length		Pitch <i>P</i>	Outside diameter <i>D</i>		
<i>d</i>	Tolerance	<i>L</i>	Tolerance	<i>DI</i>	Tolerance	<i>II</i>	Tolerance	<i>dI</i>	Tolerance	<i>I2</i>			Tolerance	
1800	1800	±11.5	5000	+50-25	1870	±11.5	290	+0 -5	1896	±11.5	290	+5 -0	270	2176



Figure 2. Case history described in this paper.

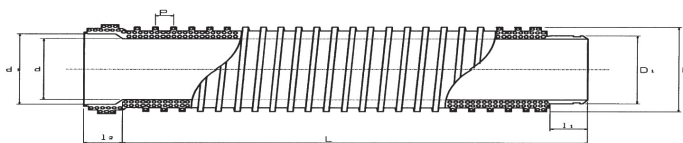


Figure 3. Geopipe used in the project.

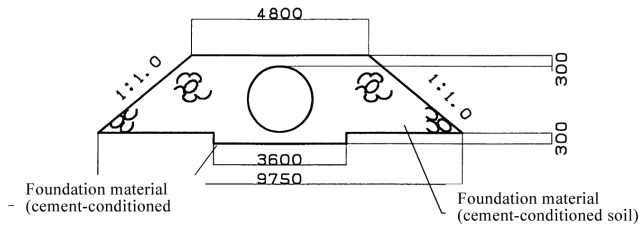


Figure 4a. Cross-section of the covering backfill in which the geopipe was embedded (all the unit in mm).

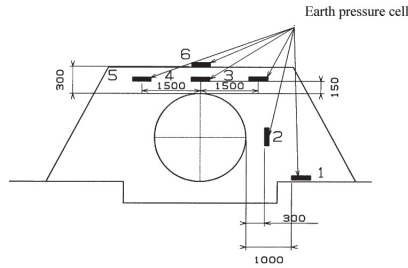


Figure 4b. Locations of earth pressure cells.

The unconfined compression strength of the backfill compacted as specified was 680 kPa.

2.2 Field measurements

A number of earth pressure cells were installed in the covering backfill surrounding the buried geopipe. The strains of the geopipe were measured by means of electric-resistance strain gauges that were attached to the internal surface of the pipe, as shown in Fig. 4b. The earth pressure and the geopipe strains were measured at the section where the total thickness of the overlying backfill became the maximum; i.e., below the crest of the road embankment (Fig. 5). The geopipe strains were measured in the longitudinal and circumferential directions of the pipe axis in at four locations (top, bottom and two sides) in the two sections. The strain data were obtained by automatic logging one time every day.

The settlements of the geopipe were measured every one meter along the center of the pipe top along the

geopipe axis as illustrated in Fig. 5. The measurement was made every one month.

2.3 Performance of the geopipe

Figure 7 shows the thickness of the overlying backfill and the settlement of the geopipe along the geopipe axis measured 19th March 2003. The ratios of the settlement to the pipe diameter (= 1.8 m) (i.e., percent deflection of the geopipe) along the geopipe axis are presented. It may be seen that the deflection of the geopipe became larger at locations where the thickness of the overlying backfill was larger. The maximum deflection in the percentage of the pipe diameter (= 1.8 m) was less than 5 percent, which is well within the allowable limit (4.56%).

The time histories of the earth pressures measured at the six locations numbered 1–6 indicated in Fig. 6 are presented in Fig. 8. The vertical earth pressures Nos. 3 through 6 measured above the geopipe are well comparable with the theoretical value according

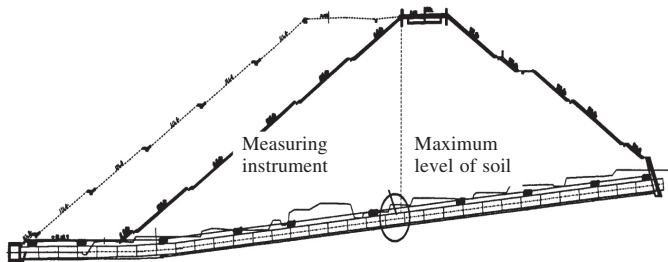


Figure 5. Cross-section of the road embankment and the location of the section where the strains and deflections of the geopipe were measured.

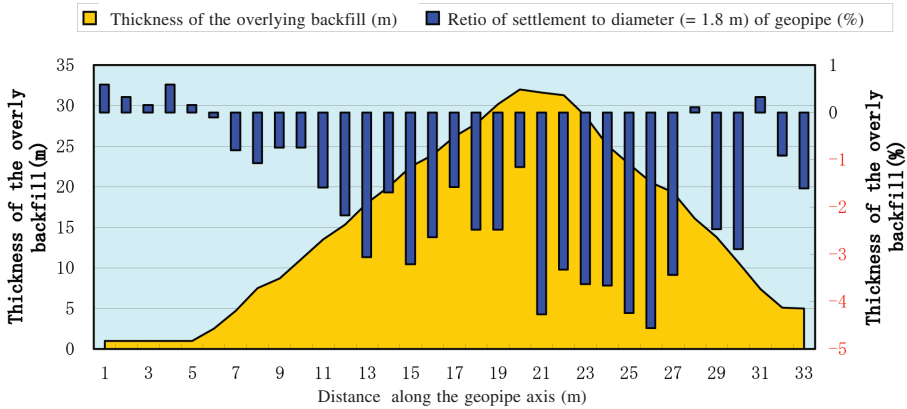


Figure 7. Thickness of the overlying backfill and the settlement of the geopipe along the geopipe axis(19th March 2003).

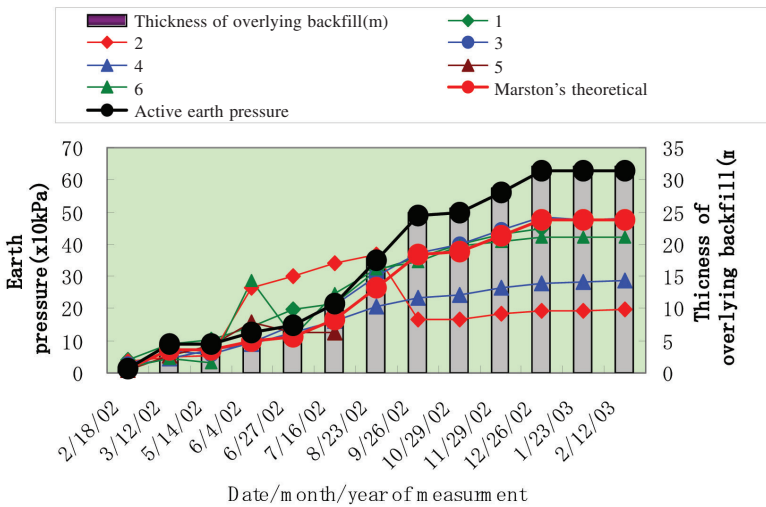


Figure 8. Measured Earth pressure and theoretical values (the numbers 1-6 indicate the locations of the earth pressure cells, Fig. 6).

to the Marston's formula (the projection type). This result indicates that the Marston's formula is relevant to the design purpose of this kind.

Figure 9 shows the time histories of the thickness of the overlying backfill and the stress (in compression) in the geopipe in the circumferential direction of the geopipe axis obtained from the strains in the geopipe. The stress at the side wall calculated by ??? and the tolerance (i.e., the allowable limit stress) are also indicated. It may be seen that the measured circumferential stress generated in the geopipe increased with an increase in the thickness of the overlying backfill but they remained within the design tolerance. Figure 10 shows the time histories of the thickness of the overlying backfill and the stress in the geopipe in the axial direction of the geopipe

obtained from the strains in the geopipe. The strains in the geopipe axis direction are much smaller than those in the circumferential direction and therefore they are far smaller than the tolerance. These observations indicate that the stress condition of the geopipe was far below the failure stress state.

Figure 11 shows the time histories of the thickness of the overlying backfill and the percent deflection (i.e., the ratio of settlement to the pipe diameter) of the geopipe at three locations Nos. 18, 20 and 23. The percent deflection of the geopipe at the three locations calculated by ??? are also presented in this figure. It may be seen that the measured values are below the calculated values, indicating that the performance of the geopipe was acceptable.

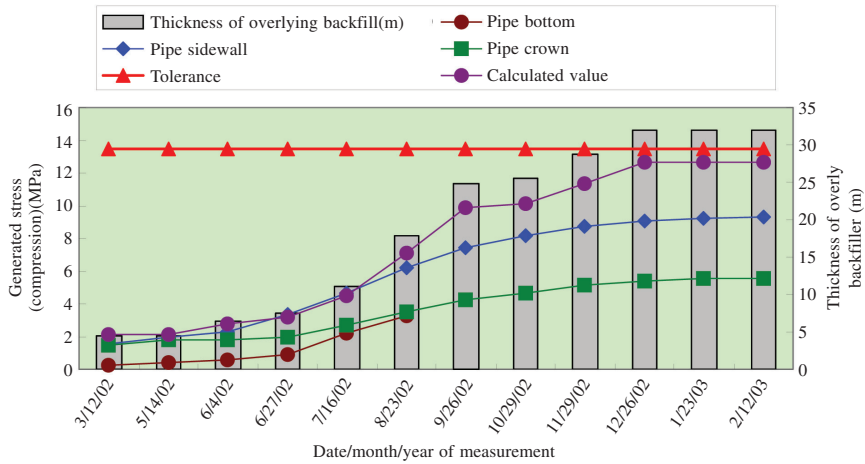


Figure 9. Time histories of the thickness of the overlying backfill and the circumferential stress in the geopipe (see Fig. 6 for the measuring locations of the geopipe strains).

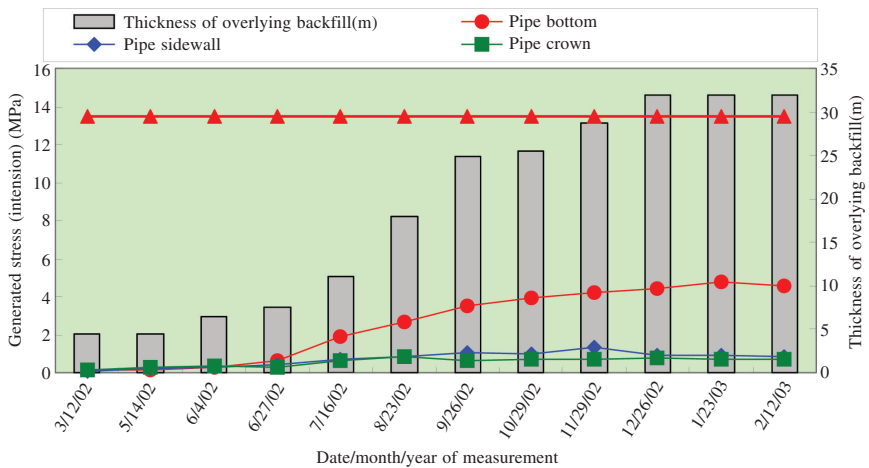


Figure 10. Time histories of the thickness of the overlying backfill and the axial stress in the geopipe (see Fig. 6 for the measuring locations of the geopipe strains).

3 CONCLUSIONS

The record of a case study of the use of a large-diameter polyethylene geopipe as a drain pipe crossing at the bottom of a high road embankment showed that the performance of the geopipe was satisfactory

as anticipated. It is of importance to note that a polyethylene pipe with a large diameter of about 2 m could be safely installed below an embankment with a total overlying backfill thickness equal to as large as 32 m.

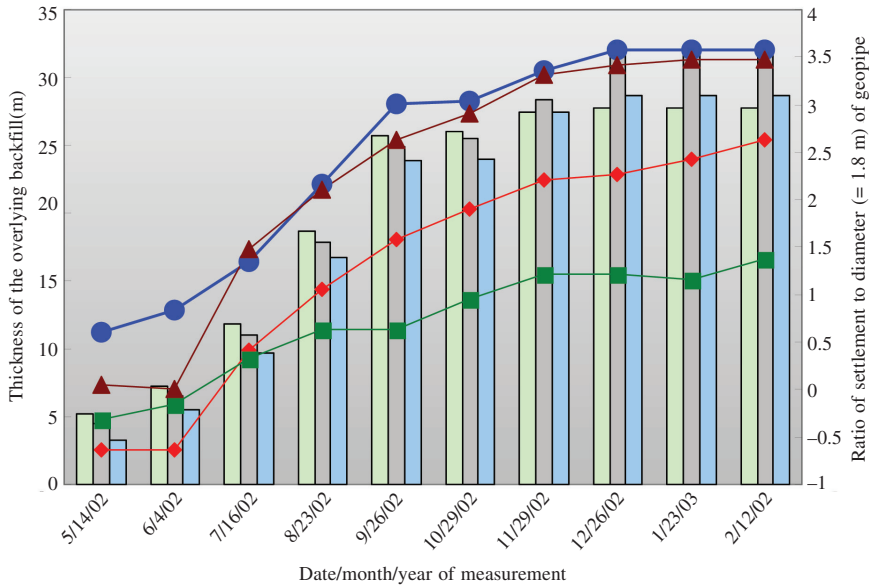
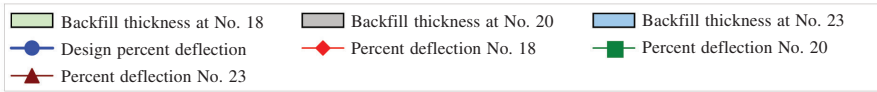


Figure 11. Time histories of the thickness of the overlying backfill and the percent deflection of the geopipe at three locations Nos. 18, 20 and 23 (Nos means the distances in m along the geopipe axis presented in Fig. 7).